Targeting PIM Kinases Affects Maintenance of CD133 Tumor Cell Population in Hepatoblastoma[1,2]

Laura L. Stafman[*], Adele P. Williams[*],
Evan F. Garner[*], Jamie M. Aye[†], Jerry E. Stewart[*],
Karina J. Yoon[‡], Kimberly Whelan[†] and
Elizabeth A. Beierle[*]

[*]Department of Surgery, University of Alabama at Birmingham, Birmingham, AL; [†]Department of Pediatrics, University of Alabama at Birmingham, Birmingham, AL; [‡]Department of Pharmacology and Toxicology, University of Alabama at Birmingham, Birmingham, AL

Abstract

Hepatoblastoma is the most common primary liver tumor in children, but treatment has not changed significantly in the past 20 years. We have previously demonstrated that Proviral Integration site for Moloney murine leukemia (PIM) kinases promote tumorigenesis in hepatoblastoma. Stem cell-like cancer cells (SCLCCs) are a subset of cells thought to be responsible for chemoresistance, metastasis, relapse, and recurrence. The aim of this study was to identify SCLCCs in hepatoblastoma and determine the role of PIM kinases in SCLCCs. Hepatoblastoma cells were separated into CD133-enriched and CD133-depleted populations and the frequency of SCLCCs was assessed. CD133 expression was determined in the presence or absence of the PIM inhibitor, AZD1208. The effects of AZD1208 on proliferation, apoptosis, and motility were assessed *in vitro* and the effect of AZD1208 on tumor growth was examined *in vivo*. We identified CD133 as a marker for SCLCCs in hepatoblastoma and showed that PIM kinases promote a SCLCC phenotype. PIM kinase inhibition with AZD1208 decreased proliferation, migration, and invasion and increased apoptosis in both SCLCCs and non-SCLCCs in a long-term passaged hepatoblastoma cell line and patient-derived xenograft. Additionally, tumor growth in mice implanted with hepatoblastoma SCLCCs was decreased with PIM inhibition such that 57% of the tumors regressed. These findings identify CD133 as a marker for SCLCCs in hepatoblastoma and provide evidence that inhibition of PIM kinases decreases stemness and tumorigenicity of SCLCCs in hepatoblastoma, making them potential therapeutic targets for the treatment of hepatoblastoma.

Translational Oncology (2019) 12, 200–208

Introduction

Hepatoblastoma is the most common primary liver tumor in children. Despite increasing incidence [1], treatment has not changed significantly since the addition of cisplatin-based therapies to treatment protocols. For those with relapsed or recurrent disease, outcomes are dismal with a 3-year overall survival of only 43% and event-free survival of 34% [2]. Additionally, chemoresistance remains a barrier to effective treatment of hepatoblastoma with 54–80% of patients developing resistance to chemotherapy after four to five cycles of treatment, leading to poor outcomes [3–5].

Stem cell-like cancer cells (SCLCCs) are a subset of cancer cells thought to play a role in metastasis, relapse, recurrence, and chemoresistance [6–9]. Their name is derived from the fact that they share many characteristics with normal tissue stem cells – self-renewal, multipotency, proliferative capacity, and dedifferentiation [10]. The specific markers to identify the SCLCC cell population in hepatoblastoma have not yet been well-defined. CD133 has been demonstrated to be a marker for SCLCCs

in multiple solid tumor types including hepatocellular carcinoma, breast cancer, colorectal cancer, and pancreatic cancer [11–14], and has been proposed as a putative marker in hepatoblastoma, but no confirmatory studies have been performed.

Proviral Integration site for Maloney murine leukemia virus (PIM) kinases are a family of serine/threonine kinases that promote tumorigenesis in a multitude of cancer types [15–21]. We have previously demonstrated that PIM inhibition decreased tumorigenesis in hepatoblastoma [22]. These data led us to hypothesize that PIM kinases may play a role in maintaining the SCLCC phenotype in hepatoblastoma and that targeting PIM kinases would decrease the phenotype *in vitro* and decrease SCLCC-enriched hepatoblastoma tumor growth *in vivo*. Given then role of CD133 in SCLCCs in other tumor types, we hypothesized that CD133 would be a marker of SCLCCs in hepatoblastoma. In this study, we identify a cell surface marker for SCLCCs in hepatoblastoma and provide evidence for the role of PIM kinases in SCLCC maintenance.

Materials and Methods

Cells and cell Culture

The human hepatoblastoma cell line, HuH6, was acquired from Thomas Pietschmann (Hannover, Germany) [23] and maintained in Dulbecco's Modified Eagle's Medium supplemented with 10% fetal bovine serum (HyClone, GE Healthcare Life Sciences, Logan, UT), 1 µg/mL penicillin/streptomycin (Gibco, Carlsbad, CA), and 2 mmol/L l-glutamine (Thermo Fisher Scientific, Waltham, MA). HuH6 cells are reported as male. The human hepatoblastoma patient-derived xenograft (PDX), COA67, was developed as described previously from a male patient [22]. Subcutaneous COA67 xenografts were harvested under sterile conditions and dissociated to a single cell solution using the Tumor Dissociation Kit, human (Miltenyi, Bergisch Gladbach, Germany) according to the manufacture's protocol and maintained in Dulbecco's Modified Eagle's Medium/Ham's F12 supplemented with 2 mmol/L l-glutamine (Thermo Fisher Scientific), 1 µg/mL penicillin/streptomycin (Gibco), 20 ng/mL epidermal growth factor (EMD Millipore, Billerica, MA), 20 ng/mL beta-fibroblast growth factor (EMD Millipore), 2% B27 supplement (Gibco), and 2.5 µg/mL amphotericin B (HyClone). Both cell lines were verified within the past 12 months using short tandem repeat analysis (Heflin Center for Genomic Sciences, University of Alabama, Birmingham (UAB), Birmingham, AL) and the long-term passaged cell line, HuH6, was determined to be free of *Mycoplasma*. Real-time qPCR assessing the frequency of human *versus* mouse actin was performed to ensure that the COA67 cells did not contain contamination from mouse cells (TRENDD RNA/DNA Isolation and TaqMan QPCR/Genotyping Core Facility, UAB, Birmingham, AL).

Antibodies and Reagents

Mouse monoclonal anti-CD133 (ab19898), anti-nestin (ab22035), and anti-Oct4 (ab18976) were from Abcam (Cambridge, MA). Rabbit polyclonal anti-PARP (9542) and anti-vinculin (4650) were from Cell Signaling Technology (Beverly, MA). Mouse monoclonal anti-β-actin (A1978) was from Sigma Aldrich (St. Louis, MO). AZD1208 was obtained from Cayman Chemical (Ann Arbor, MI).

Separation of Cells into CD133-Enriched and CD133-Depleted Populations

Cells were separated into CD133-enriched or CD133-depleted populations based on the cell surface expression of CD133. The CD133 MicroBead Kit – Tumor Tissue, human (Miltenyi) was utilized according to manufacturer's protocol. Briefly, cells were incubated with FcR Blocking Reagent followed by magnetic CD133 MicroBeads for 20 minutes at 4 °C. Cells were washed with buffer and placed onto LS (HuH6 cells) or MS (COA67 cells) magnetic columns (Miltenyi) and placed in the magnetic field of a MACS Separator. The flow-through containing unlabeled cells was collected as CD133-depleted cells. After washing the column with buffer three times, the column was removed from the magnetic field. Magnetically labeled cells were flushed from the column using a plunger and collected as CD133-enriched cells.

In Vitro Limiting Dilution Sphere Assay

To determine the ability of cells to form spheres, *in vitro* limiting dilution assays were performed. Cells were plated into 96 well ultra-low attachment plates using serial dilutions with 5000, 1000, 500, 100, 50, 20, or 1 cell per well for HuH6 cells and 50,000, 10,000, 5000, 1000, 500, 100, 50, or 1 cell per well for COA67 cells with at least 10 replicates per dilution. Cells were plated into Dulbecco's Modified Eagle's Medium/Ham's F12 supplemented with 2 mmol/L l-glutamine (Thermo Fisher Scientific), 1 µg/mL penicillin/strepto-mycin (Gibco), 20 ng/mL epidermal growth factor (EMD Millipore), 20 ng/mL beta-fibroblast growth factor (EMD Millipore), 2% B27 supplement (Gibco), and 2.5 µg/mL amphotericin B (HyClone) combined with 50% conditioned medium of the same composition from the same cell line. The conditioned media was harvested after 24–48 hours of culture with healthy cells and after removal of cells by centrifugation, the conditioned media was sterile filtered. Once spheres were present in the wells containing the most cells, all wells were counted. The presence or absence of spheres in each well was determined by a single researcher. Extreme limiting dilution analysis software was utilized to analyze the data (http://bioinf.wehi.edu.au/software/elda/).

Immunoblotting

Whole-cell lysates were isolated in radioimmunoprecipitation (RIPA) buffer supplemented with protease inhibitors (Sigma Aldrich), phosphatase inhibitors (Sigma Aldrich), and phenylmetha-nesulfonylfluoride (Sigma Aldrich). Lysates were centrifuged at 14000 rpm for 30 minutes at 4 °C. Protein concentrations were determined using Pierce BCA Protein Assay (Thermo Fisher Scientific) and separated by electrophoresis on sodium dodecyl sulfate polyacrylamide (SDS-PAGE) gels. Molecular weight markers (Precision Plus Protein Kaleidoscope, Bio-Rad, Hercules, CA) were used to confirm the expected size of the proteins of interest. Immunoblots were developed with Luminata Classico or Crescendo Western HRP Substrate (EMD Millipore) using film. Blots were stripped with stripping solution (Bio-Rad) at 65 °C for 20 minutes and then re-probed with selected antibodies. Equal protein loading was confirmed using β-actin or vinculin. Densitometry was performed using Scion Image Program. Each band was normalized to background on the blot, and then normalized to their respective actin band. All bands were compared to the 0 µM treatment group, which was given the value of 1 as previously reported [24].

Proliferation Assay

To establish the effects of AZD1208 on proliferation, the CellTiter 96 Aqueous Non-Radioactive Cell Proliferation Assay (Promega, Madison, WI) was utilized. CD133-enriched or CD133-depleted HuH6 or COA67 cells (5×10^3 per well) were plated in 96-well plates and treated

with AZD1208 for 24 hours. Following treatment, 10 μL of CellTiter 96 reagent was added to each well and the absorbance was read at 490 nm using a microplate reader (BioTek Gen5, Winooski, VT). Background absorbance of media alone was subtracted and proliferation was reported as fold change.

Migration and Invasion

To determine the effects of AZD1208 treatment on cell movement, migration and invasion assays were performed. For migration assays, 24-well culture plates with 8 μm micropore Transwell inserts (Corning Life Sciences, Corning, NY) were utilized. The bottoms of the inserts were coated with collagen I (10 μg/mL, MP Biomedicals, Santa Ana, CA) for HuH6 studies or fibronectin (10 μg/mL, Qiagen, Germantown, MD) for COA67 studies overnight at 37 °C and then washed with phosphate-buffered saline (PBS). The inserts were then placed in wells containing 333 μL media with the appropriate concentration of AZD1208. CD133-enriched or CD133-depleted cells (3×10^4 HuH6 or 3×10^5 COA67) were placed inside each insert in media containing the appropriate concentration of AZD1208 and allowed to migrate for 24 or 72 hours (HuH6 and COA67, respectively). Inserts were fixed with 3% paraformaldehyde and stained with 1% crystal violet. Images were obtained using a light microscope and the percent of the insert area covered

with cells was determined using ImageJ (https://imagej.nih.gov/ij). Migration was reported as fold change in percent of insert area covered with migrated cells.

Invasion was assessed in a similar manner. The insides of the inserts were coated with Matrigel (1 mg/mL, 50 μL; BD Biosciences, Franklin Lakes, NJ) overnight at 37 °C and then washed with PBS. For COA67 invasion studies, the bottoms of the inserts were coated with fibronectin (10 μg/mL, Qiagen) overnight at 37 °C. The inserts were then placed in wells containing 333 μL media with the appropriate concentration of AZD1208. CD133-enriched or CD133-depleted cells (3×10^4 HuH6 or 3×10^5 COA67) were placed inside each insert in media containing the appropriate concentration of AZD1208 and allowed to invade for 24 or 72 hours (HuH6 and COA67, respectively). Fixation, staining, image acquisition, quantification, and reporting of invasion were performed as described above for migration studies.

In Vivo Studies

Six-week-old female athymic nude mice (Envigo, Pratville, AL) were maintained in a pathogen-free facility with static conventional housing, standard 12-hour light/dark cycles, and *ad libitum* access to Harlan Rodent Diet Teklad 4% fat mouse/rat chow (Envigo) and water. Experiments were approved by the University of Alabama,
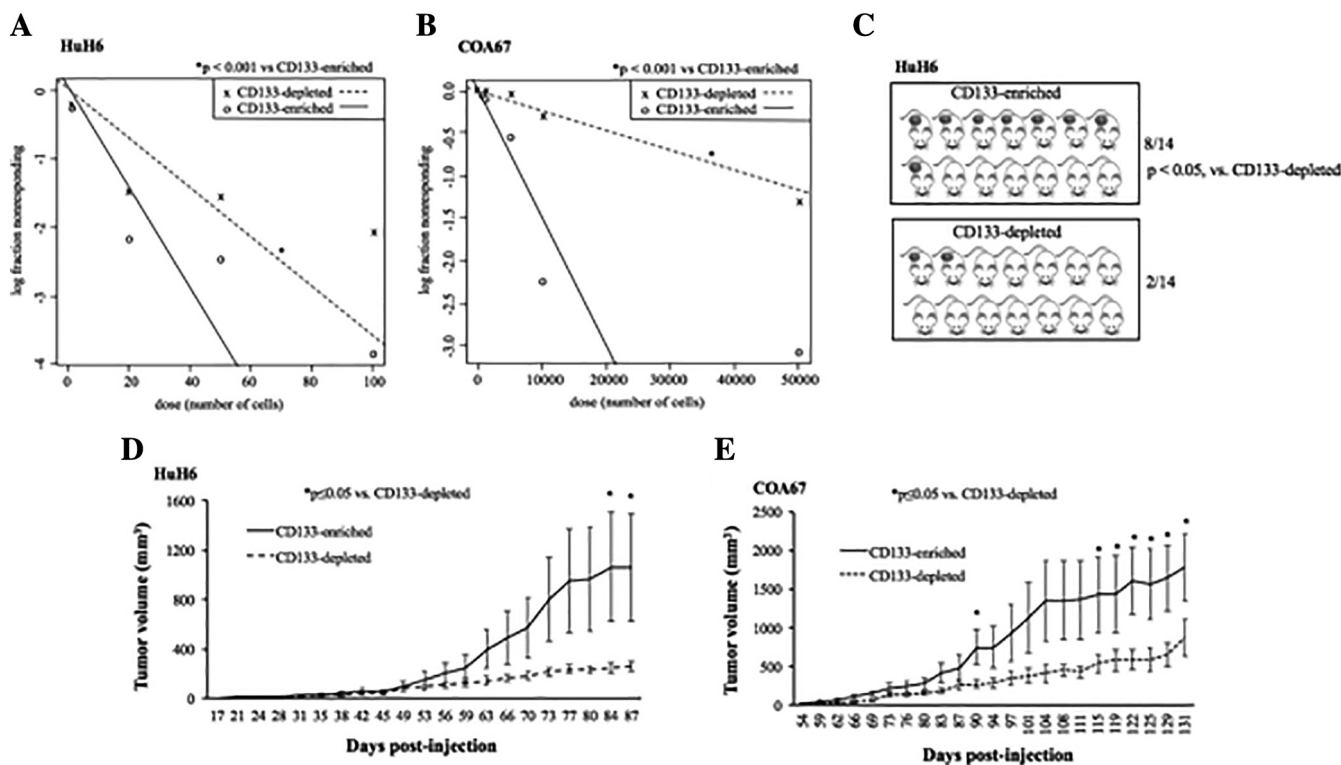
Figure 1. CD133 is a marker for SCLCCs in hepatoblastoma. *In vitro* sphere formation assays were used to assess the frequency of SCLCCs in CD133-enriched *versus* CD133-depleted (A) HuH6 and (B) COA67 hepatoblastoma cell populations. Cells were plated in serial dilution in serum-free media. Once spheres were present, the presence or absence of spheres in each well was determined and data analyzed using extreme limiting dilution analysis software (http://bioinf.wehi.edu.au/software/elda/). CD133-enriched hepatoblastoma cells formed spheres more readily than CD133-depleted hepatoblastoma cells in both the HuH6 cell line and COA67 PDX cells. (C) *In vivo* tumorigenic assays were used to assess the ability of CD133-enriched *versus* CD133-depleted hepatoblastoma cells to form tumors in mice. Three weeks after injection of 5×10^4 cells, 8/14 mice injected with CD133-enriched HuH6 cells bore tumors and 2/14 mice injected with CD133-depleted HuH6 cells bore tumors ($P = .02$). (D) Animals injected with CD133-enriched HuH6 cells (5×10^4) grew tumors that were significantly larger than animals that were injected with CD133-depleted (5×10^4) HuH6 cells ($P \leq .05$). (E) Animals were injected with 1×10^6 CD133-enriched or CD133-depleted COA67 cells. Tumors that formed in the animals with CD133-enriched cells were significantly larger than CD133-depleted COA67 tumors ($P \leq .05$).

Birmingham, Institutional Animal Care and Use Committee (IACUC-9803) and conducted within institutional, national, and international guidelines. Tumor volumes were measured with calipers twice weekly and calculated using the formula (width^2 × length)/2, where the length is the largest measurement [25].

In vivo limiting dilution assays were employed to determine tumorigenicity. For the HuH6 *in vivo* tumorigenic assay, 5×10^4 cells were injected subcutaneously in the right flank of 28 female athymic nude mice (n = 14 CD133-enriched; n = 14 CD133-depleted), and animals were followed for tumor growth. For the COA67 *in vivo* tumorigenic assay, 1×10^6 cells were injected subcutaneously in the right flank of 14 female athymic nude mice (n = 7 CD133-enriched; n = 7 CD133-depleted) and animals were followed for tumor growth.

For the AZD1208 *in vivo* study, 5×10^4 cells were injected subcutaneously in the right flank of 28 female athymic nude mice (n = 14 CD133-enriched; n = 14 CD133-depleted). Six weeks after

injection, when tumors reached an average of approximately 50 mm^3, mice within each group were randomized to receive vehicle (n = 7 each group; ORA-Plus, 50 μL; Perrigo, Allegan, MI) or AZD1208 (n = 7 each group; 30 mg/kg body weight/day in ORA-Plus, 50 μL) by oral gavage. Mice bearing CD133-enriched HuH6 tumors were treated for 40 days and mice bearing CD133-depleted HuH6 tumors were treated for 77 days. Treatment was given during the animals' light cycle. Animals were humanely euthanized when IACUC parameters were reached or 45 weeks after injection for those that did not reach IACUC parameters before that time. Tumors were harvested and dissociated and *in vivo* sphere forming assays were performed as above. Flow cytometry for detection of CD133 expression was performed as described below.

Flow Cytometry

Flow cytometry was utilized to establish the effects of AZD1208 upon CD133 expression. Cells were labeled with human CD133/1
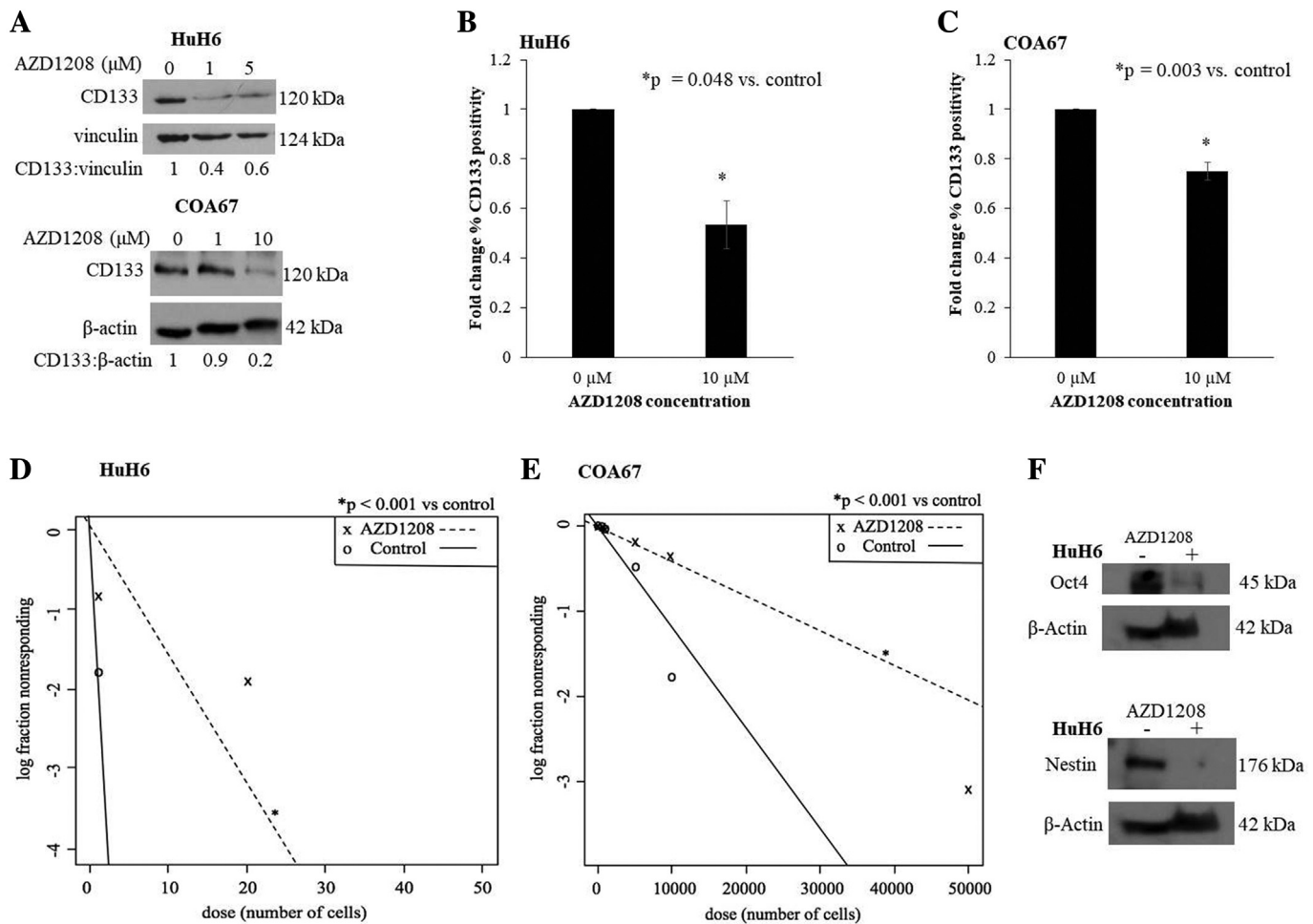
Figure 2. PIM inhibition decreased CD133 expression in hepatoblastoma cells and decreased sphere formation and other stemness markers in CD133-enriched hepatoblastoma cells. HuH6 and COA67 cells were treated for 24 hours with increasing concentrations of AZD1208. Immunoblotting of whole cell lysates of (A) HuH6 and COA67 cells revealed a decrease in CD133 expression with AZD1208 treatment. Densitometry was utilized to evaluate the bands, providing confirmatory evidence that AZD1208 decreased CD133 expression. CD133 expression was also evaluated by FACS. AZD1208 significantly decreased CD133 expression in both (B) HuH6 cells and (C) COA67 cells. HuH6 and COA67 cells were treated with 10 μM AZD1208 and sphere forming assays were performed. AZD1208 significantly reduced sphere formation in CD133-enriched (D) HuH6 and (E) COA67 cells. (F) HuH6 CD133-enriched cell populations were treated with 20 μM AZD1208 for 24 hours and whole cell lysates examined for the differentiation markers Oct4 and nestin. AZD1208 led to decreased expression of Oct4 and nestin, indicating a loss of stemness.

(AC133)-APC antibody (Miltenyi) according to the manufacturer's instructions. Unlabeled cells were used as controls. The percent of cells positive for APC was determined *via* flow cytometry using the BD FACSCalibur platform (BD Biosciences, Franklin Lakes, NJ). All analyses were performed using FlowJo software (BD Biosciences). For the permeabilized studies, cells were fixed with ethanol and then permeabilized with 0.1% Triton-X for 15 minutes in the dark prior to labeling.

Results

CD133 is a Marker for SCLCCs in Human Hepatoblastoma

To determine whether CD133 served as a marker of SCLCCs in hepatoblastoma, we investigated tumor forming capacity. HuH6 and COA67 human hepatoblastoma cells were separated into CD133-enriched and CD133-depleted populations. When cultured in serum- and attachment-free conditions, the CD133-enriched population formed spheres at lower cell concentrations than CD133-depleted in both HuH6 and COA67 cells (Figure 1, *A* and *B*), indicating a more SCLCC phenotype in the enriched population. Using *in vivo* tumorigenic assays, CD133-enriched or CD133-depleted cells were injected subcutaneously in the flank of athymic nude mice and tumor growth was monitored. Three weeks after injection, 8 of the 14 mice injected with CD133-enriched HuH6 cells bore tumors whereas 2 of the 14 mice injected with CD133-depleted HuH6 cells bore tumors ($P = .02$, Figure 1*C*). Additionally, the average tumor volume in mice injected with CD133-enriched HuH6 cells was significantly greater than that in mice injected with CD133-depleted HuH6 cells ($P \leq .05$, Figure 1*D*). Tumors in mice injected with CD133-enriched COA67 cells were also significantly larger than those in mice injected with

CD133-depleted COA67 cells ($P \leq .05$, Figure 1*E*). Cells passaged in mice in the *in vivo* tumorigenic assays retained their differential stemness profiles throughout the course of the experiment. Cell surface expression of CD133 tended to be lower in the CD133-depleted groups than CD133-enriched groups (Supplemental Figure 1, *A* and *B*) and cells from CD133-enriched tumors formed spheres at significantly lower cell concentrations than cells from CD133-depleted tumors (Supplemental Figure 1, *C* and *D*).

PIM Inhibition Decreased CD133 Expression in Hepatoblastoma Cells and Decreased Sphere Formation and Other Stemness Markers in CD133-Enriched Hepatoblastoma Cells

As we have previously shown that PIM kinase inhibition decreases tumorigenicity in hepatoblastoma [22], we wished to determine whether the selective pan-PIM inhibitor, AZD1208 [26], may have an effect on the SCLCC phenotype. Treatment of HuH6 and COA67 cells with AZD1208 decreased CD133 expression as measured by Western blotting (Figure 2*A*) and flow cytometry for CD133 expression in permeabilized cells (Figure 2, *B* and *C*). Additionally, there was a decrease in sphere formation (Figure 2, *D* and *E*). All of these findings indicated a decrease in the SCLCC phenotype following PIM inhibition. Oct4 and nestin have been shown to be markers of stemness in many cancer types [27–30] including hepatocellular carcinoma [31,32], so we studied whether PIM inhibition affected these markers in hepatoblastoma. When investigating the CD133-enriched cells alone, AZD1208 treatment decreased expression of the stemness markers, Oct4 and nestin, in HuH6 cells (Figure 2*F*), providing further data that PIM supports the SCLCC phenotype in hepatoblastoma.
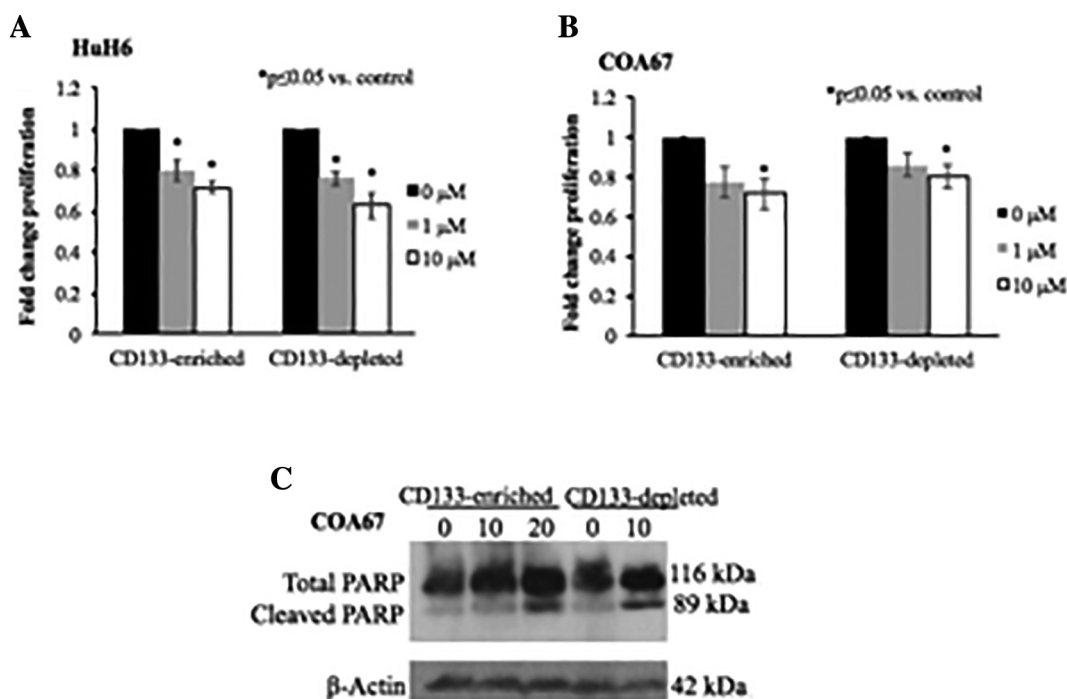
Figure 3. PIM inhibition decreased proliferation and induced apoptosis in CD133-enriched and CD133-depleted hepatoblastoma cells. CD133-enriched and CD133-depleted populations of HuH6 and COA67 cells were treated with increasing concentrations of AZD1208 for 24 hours. Proliferation was assessed with CellTiter 96 assay. AZD1208 decreased proliferation in both CD133-enriched and CD133-depleted (A) HuH6 and (B) COA67 cells. The CD133-enriched and CD133-depleted COA67 cell population was treated with AZD1208 (0, 10, or 20 μM) for 24 hours and whole cell lysates obtained. (C) Immunoblotting revealed an increased in cleaved PARP, indicating apoptosis, in both CD133-enriched and CD133-depleted COA67 cell populations.

PIM Inhibition Decreased Proliferation, Induced Apoptosis, and Decreased Motility in CD133-Enriched and CD133-Depleted Hepatoblastoma Cells

With the knowledge that PIM inhibition decreased the stem-like phenotype of hepatoblastoma cells, we wished to assess the effects of PIM inhibition on proliferation, apoptosis, and motility in CD133-enriched *versus* CD133-depleted hepatoblastoma cells. Both the HuH6 and COA67 CD133-enriched and CD133-depleted populations exhibited decreased cell proliferation in the presence of AZD1208 ($P \le .05$, Figure 3, *A* and *B*). Using immunoblotting, an increase in cleaved PARP was observed in both CD133-enriched and CD133-depleted populations of COA67 cells (Figure 3*C*), indicative of induction of apoptosis with PIM inhibition. Motility was decreased in both CD133-enriched and CD133-depleted HuH6 and COA67 cells. There was a decrease in migration in both CD133-enriched and CD133-depleted HuH6 and COA67 cells (Figure 4, *A* and *B*) as well as a decrease in invasion in both CD133-enriched and CD133-depleted HuH6 and COA67 cells (Figure 4, *C* and *D*). For the proliferation, apoptosis, and motility assays, the CD133-enriched population was affected in a similar manner as the CD133-depleted population, indicating that the CD133-enriched population was not resistant to PIM inhibition.
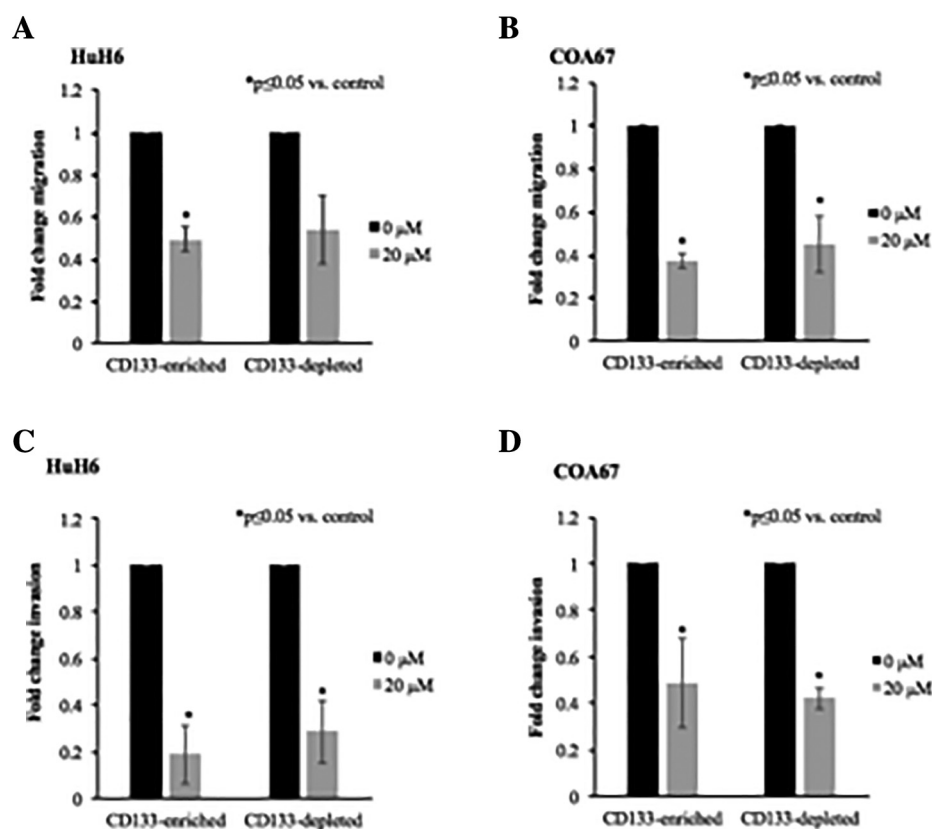
PIM Inhibition Decreased CD133-Enriched HuH6 Tumor Growth in Mice and Decreased Stemness In Vivo

Studies were then advanced to an *in vivo* model. Fourteen mice were injected subcutaneously with CD133-enriched HuH6 cells and randomized to receive either vehicle or AZD1208 by oral gavage daily for 40 days. Mice treated with AZD1208 had significantly smaller tumors than vehicle-treated mice ($P \le .05$, Figure 5*A*). Additionally, four of the seven mice treated with AZD1208 bearing CD133-enriched hepatoblastoma tumors experienced complete regression of their tumor, even after the treatment concluded (Supplemental Figure 2). A similar study was performed using CD133-depleted HuH6 cells, but there was no significant difference between tumor volume between the groups receiving vehicle or AZD1208 (Supplemental Figure 3*A*). At the time of euthanasia, tumors were harvested and sphere formation assays were performed. Cells from mice bearing CD133-enriched tumors treated with AZD1208 required higher cell concentrations to form spheres ($P \le .001$, Figure 5*B*), indicating a lower frequency of SLCCs in the treated tumors. In both the CD133-enriched and depleted tumors, AZD1208 treatment resulted in areas of tumor necrosis (Figure 5*C* and Supplemental Figure 3*B*).

Discussion

We report for the first time that CD133 is a marker for SCLCCs in hepatoblastoma. Using both *in vitro* limiting dilution sphere formation assays and *in vivo* tumorigenic assays, we found that the CD133-enriched human hepatoblastoma cell population, both from a long-term passaged cell line and a human PDX, formed spheres in culture and tumors in mice more readily than the CD133-depleted cell population. Both sphere formation and *in vivo* tumorigenicity are indicative of the presence of SCLCCs and these two studies serve as the gold standard for identifying markers for SCLCCs [33,34]. CD133 has

Figure 4. PIM inhibition decreased motility in CD133-enriched and CD133-depleted hepatoblastoma cells. Migration and invasion were measured with modified Boyden chambers. Treatment of CD133-enriched and CD133-depleted cells with AZD1208 (20 μM) for 72 hours resulted in decreased migration in (A) HuH6 and (B) COA67 cells and invasion in (C) HuH6 and (D) COA67 cells compared to untreated cells. Migration in the CD133-depleted HuH6 cell population was decreased compared to control, but did not reach statistical significance.
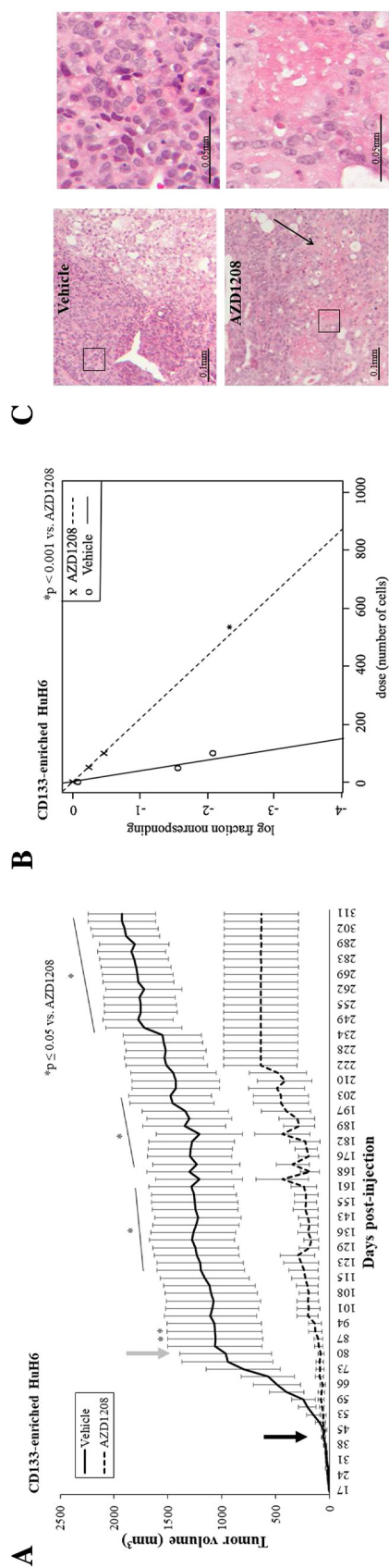
Figure 5. PIM inhibition decreased CD133-enriched HuH6 tumor growth in mice and decreased stemness *in vivo*. (A) CD133-enriched cells (5×10^4) were injected subcutaneously in the flanks of 14 athymic nude mice. On post-injection day 42 (treatment start, black arrow), mice were randomized to receive vehicle (ORA-Plus, n = 7) or AZD1208 (30 mg/kg body weight/day in ORA-Plus, n = 7) by oral gavage for 40 days (treatment end, gray arrow). Mice treated with AZD1208 had significantly smaller tumors than those treated with vehicle ($P \le .05$). (B) Tumors were dissociated and *in vitro* sphere formation assays were performed. Cells from mice treated with AZD1208 exhibited significantly decreased sphere formation compared to cells from vehicle-treated mice ($P < .001$). (C) Representative photomicrographs of hematoxylin and eosin staining of vehicle (*upper panels*) or AZD1208 (*lower panels*) treated CD133-enriched tumors at 10× (*left panels*) and 40× (*right panels*). Treatment with AZD1208 resulted in large areas of necrosis in the tumors (*black arrow, lower left panel*).

been described as a marker for SCLCCs in multiple other cancer types including hepatocellular carcinoma [11,35], but it has not been proven to identify SCLCCs in hepatoblastoma. Ma et al. characterized CD133 as a marker for tumorigenic liver cancer stem/progenitor cells, but their focus was on hepatocellular carcinoma as opposed to hepatoblastoma. The one cell line that was used to examine hepatoblastoma in that study, HepG2, has since been determined to represent hepatocellular carcinoma based on gene expression studies [36]. Our finding that CD133 is a marker for SCLCCs in hepatoblastoma is consistent with others' findings that CD133 expression portends poor prognosis in hepatoblastoma. Bahnassy et al. found that CD133 expression correlated with advanced stage disease, reduced overall survival, reduced disease-free survival, and poor response to treatment in human hepatoblastoma tumors specimens [37].

Knowledge that CD133 is a marker for SCLCCs in hepatoblastoma may have important therapeutic implications. Investigators may now justify separation of cell populations into CD133-enriched (SCLCCs) or CD133-depleted cell populations (non-SCLCCs), for further study to understand how to better target this particular cell population in hepatoblastoma. Researchers have been examining mechanisms to specifically target SCLCCs utilizing CD133. Anti-CD133 single-chain variable fragment conjugated targeted toxins, bispecific antibodies, and antibody-conjugated nanoparticles containing chemotherapy drugs have been examined, but their use in solid tumors has proven challenging given limited delivery due to heterogeneous vascularity and hypoperfusion [38,39]. Another potential mechanism to target cells bearing CD133 on their surface is natural killer cells targeting CD133 [38], but again, issues remain in delivery to solid tumors given the immunosuppressive tumor microenvironment [40]. More recently, researchers have begun to design autologous chimeric antigen receptor-modified (CAR) T cells targeting CD133. A phase I clinical trial in 23 patients with hepatocellular, pancreatic, and colorectal carcinomas showed the feasibility and effective activity of these CAR T cells targeting CD133 [41]. Many of the issues that have been observed with CAR T cells targeting other molecules were also observed in this trial, namely "on-target, off-tumor" effects including hematopoietic systemic toxicity and bilirubinemia. Despite these side effects, CAR T cells directed toward CD133 hold promise for the treatment of hepatoblastoma.

Given these challenges to targeting CD133 directly, we examined the effect of AZD1208 on hepatoblastoma cells to determine whether small molecule PIM inhibition therapy may be able to target SCLCCs. We found that AZD1208 treatment of bulk (unsorted) hepatoblastoma cells decreased CD133 expression and sphere formation, indicating a decrease in the stem-like phenotype. Additionally, in the CD133-enriched population specifically, there was a decrease in stemness with PIM inhibition, indicated by a decrease in Oct4 and nestin. While Oct4 and nestin not previously been demonstrated to be markers of stemness in hepatoblastoma, they are known markers of stemness in many cancer types [27–30] including hepatocellular carcinoma [31,32]. Given that the CD133-enriched population specifically exhibited a decrease in stemness with PIM inhibition, we proposed that PIM inhibition would have an anti-tumor effect on both the CD133-enriched and the CD133-depleted cell populations. SCLCCs are known to play a significant role in chemoresistance [42,43], so demonstrating that AZD1208 affected this subpopulation is promising as AZD1208 may be employed as a novel therapeutic to eradicate the cells that have evaded traditional chemotherapy.

We examined the phenotypic effects of PIM inhibition on the SCLCC *versus* non-SCLCC populations to determine whether

hepatoblastoma SCLCCs exhibited resistance to PIM kinases. We have previously demonstrated that PIM kinases, specifically PIM3, decreased hepatoblastoma proliferation and motility and induced apoptosis [22]. We showed in the current study that both SCLCCs and non-SCLCCs exhibited decreased proliferation and motility and increased apoptosis with PIM inhibition. These findings are depicted in Supplemental Figure 4 and indicate that hepatoblastoma SCLCCs may not have the capacity to evade the effects of PIM kinase inhibition, again, providing data indicating that AZD1208 may be a promising drug to eradicate hepatoblastoma SCLCCs and potentially decrease tumor recurrence and chemoresistance.

Using an *in vivo* xenograft model, we showed that PIM inhibition decreased the growth of tumors comprised of hepatoblastoma CD133-enriched cells, with 57% of the animals experiencing complete tumor regression. A similar response to PIM inhibition was expected in non-SCLCCs *in vivo* given the results observed *in vitro*. There was a trend toward decreased tumor volume in these animals treated with AZD1208, but it did not reach statistical significance. This difference between the SCLCC and non-SCLCC results *in vivo* may be explained by the effect of PIM inhibition on the SCLCC tumor microenvironment in addition to the tumor cells themselves. Cancer stem cells reside within a specialized microenvironment that functions to regulate their stemness [44] and changing the microenvironment *via* PIM inhibition may function to further decrease the SCLCC phenotype. PIM kinase inhibition has been shown to decrease CXCR4 surface expression and phosphorylation in leukemia cells [45]. CXCR4 functions as the ligand for CXCL12, which is expressed by a multitude of cell types in the microenvironment. The CXCR4 / CXCL12 interaction between tumor cells and the microenvironment establish and support the immunosuppressive and angiogenic nature of the microenvironment [46–48]. Therefore, in the animals injected with the SCLCC population, PIM kinase inhibition may have had an additional effect upon the interaction between cancer cells and the microenvironment than in the animals bearing tumors from the non-SCLCC population.

Current treatment of hepatoblastoma involves a combination of chemotherapy drugs in which cisplatin is the backbone. The addition of AZD1208 to cisplatin treatment has been demonstrated to decrease tumor growth more than cisplatin alone in a mouse model of hepatoblastoma [22]. Those findings may be explained by our results described here regarding the preferential targeting of SCLCCs by PIM inhibition. Cisplatin enriches the frequency of cancer stem cells in hepatocellular carcinoma [49]. By giving cisplatin to target the non-SCLCCs and increase the frequency of SCLCCs alongside AZD1208 to target the SCLCCs, we may be able to more effectively treat hepatoblastoma and eradicate SCLCCs. These topics will be the focus of future studies.

In summary, these data demonstrate for the first time that CD133 is a marker for SCLCCs in hepatoblastoma. Additionally, PIM inhibition decreased stemness in bulk and SCLCCs and tumorigenicity in SCLCCs. These results suggest that PIM inhibitors may be useful as a novel therapeutic target to treat hepatoblastoma and decrease its recurrence through the targeting of SCLCCs.

Supplementary data to this article can be found online at https://doi.org/10.1016/j.tranon.2018.10.008.

Author Contributions
Stafman was involved in study concept and design, data collection, data analysis, and manuscript preparation. Williams, Garner, Aye, and Stewart contributed with data collection and analysis. Yoon and Whelan were involved in the development and propagation of the patient-derived xenograft. Beierle provided senior guidance with study concept and design, data analysis, and manuscript preparation.

References

[1] Linabery AM and Ross JA (2008). Trends in childhood cancer incidence in the US (1992-2004). *Cancer* **112**(2), 416–432.

[2] Semeraro M, Branchereau S, Maibach R, Zsiros J, Casanova M, Brock P, Domerg C, Aronson DC, Zimmermann A, and Laithier V, et al (2013). Relapses in hepatoblastoma patients: clinical characteristics and outcome–experience of the International Childhood Liver Tumour Strategy Group (SIOPEL). *Eur J Cancer* **49**(4), 915–922.

[3] von Schweinitz D, Byrd DJ, Hecker H, Weinel P, Bode U, Bürger D, Erttmann R, Harms D, and Mildenberger H (1997). Efficiency and toxicity of ifosfamide, cisplatin and doxorubicin in the treatment of childhood hepatoblastoma. Study Committee of the Cooperative Paediatric Liver Tumour Study HB89 of the German Society for Paediatric Oncology and Haematology. *Eur J Cancer* **33**(8), 1243–1249.

[4] von Schweinitz D, Hecker H, Harms D, Bode U, Weinel P, Bürger D, Erttmann R, and Mildenberger H (1995). Complete resection before development of drug resistance is essential for survival from advanced hepatoblastoma — a report from the German Cooperative Pediatric Liver Tumor Study HB-89. *J Pediatr Surg* **30** (6), 845–852.

[5] Warmann S, Hunger M, Teichmann B, Flemming P, Gratz KF, and Fuchs J (2002). The role of the MDR1 gene in the development of multidrug resistance in human hepatoblastoma: clinical course and in vivo model. *Cancer* **95**(8), 1795–1801.

[6] Alisi A, Cho WC, Locatelli F, and Fruci D (2013). Multidrug resistance and cancer stem cells in neuroblastoma and hepatoblastoma. *Int J Mol Sci* **14**(12), 24706–24725.

[7] Peitzsch C, Tyutyunnykova A, Pantel K, and Dubrovska A (2017). Cancer stem cells: The root of tumor recurrence and metastases. *Semin Cancer Biol* **44**, 10–24.

[8] Chang JC (2016). Cancer stem cells: Role in tumor growth, recurrence, metastasis, and treatment resistance. *Medicine (Baltimore)* **95**(1 Suppl. 1), S20–S25.

[9] Kruger JA, Kaplan CD, Luo Y, Zhou H, Markowitz D, Xiang R, and Reisfeld RA (2006). Characterization of stem cell-like cancer cells in immune-competent mice. *Blood* **108**(12), 3906–3912.

[10] Shipitsin M and Polyak K (2008). The cancer stem cell hypothesis: in search of definitions, markers, and relevance. *Lab Invest* **88**(5), 459–463.

[11] Ma S, Chan KW, Hu L, Lee TK, Wo JY, Ng IO, Zheng BJ, and Guan XY (2007). Identification and characterization of tumorigenic liver cancer stem/ progenitor cells. *Gastroenterology* **132**(7), 2542–2556.

[12] Wright MH, Calcagno AM, Salcido CD, Carlson MD, Ambudkar SV, and Varticovski L (2008). Brca1 breast tumors contain distinct CD44+/CD24- and CD133+ cells with cancer stem cell characteristics. *Breast Cancer Res* **10**(1), R10.

[13] Ren F, Sheng WQ, and Du X (2013). CD133: a cancer stem cells marker, is used in colorectal cancers. *World J Gastroenterol* **19**(17), 2603–2611.

[14] Hermann PC, Huber SL, Herrler T, Aicher A, Ellwart JW, Guba M, Bruns CJ, and Heeschen C (2007). Distinct populations of cancer stem cells determine tumor growth and metastatic activity in human pancreatic cancer. *Cell Stem Cell* **1**(3), 313–323.

[15] Möröy T, Grzeschiczek A, Petzold S, and Hartmann KU (1993). Expression of a Pim-1 transgene accelerates lymphoproliferation and inhibits apoptosis in lpr/lpr mice. *Proc Natl Acad Sci U S A* **90**(22), 10734–10738.

[16] Möröy T, Verbeek S, Ma A, Achacoso P, Berns A, and Alt F (1991). E mu N- and E mu L-myc cooperate with E mu pim-1 to generate lymphoid tumors at high frequency in double-transgenic mice. *Oncogene* **6**(11), 1941–1948.

[17] Yan B, Yau EX, Samanta S, Ong CW, Yong KJ, Ng LK, Bhattacharya B, Lim KH, Soong R, and Yeoh KG, et al (2012). Clinical and therapeutic relevance of PIM1 kinase in gastric cancer. *Gastric Cancer* **15**(2), 188–197.

[18] Weirauch U, Beckmann N, Thomas M, Grünweller A, Huber K, Bracher F, Hartmann RK, and Aigner A (2013). Functional role and therapeutic potential of the pim-1 kinase in colon carcinoma. *Neoplasia* **15**(7), 783–794.

[19] Santio NM, Eerola SK, Paatero I, Yli-Kauhaluoma J, Anizon F, Moreau P, Tuomela J, Härkönen P, and Koskinen PJ (2015). Pim kinases promote migration and metastatic growth of prostate cancer xenografts. *PLoS One* **10**(6) e0130340.

[20] Wu Y, Wang YY, Nakamoto Y, Li YY, Baba T, Kaneko S, Fujii C, and Mukaida N (2010). Accelerated hepatocellular carcinoma development in mice expressing the Pim-3 transgene selectively in the liver. *Oncogene* **29**(15), 2228–2237.

[21] Narlik-Grassow M, Blanco-Aparicio C, and Carnero A (2014). The PIM family of serine/threonine kinases in cancer. *Med Res Rev* **34**(1), 136–159.

[22] Stafman LL, Mruthyunjayappa S, Waters AM, Garner EF, Aye JM, Stewart JE, Yoon KJ, Whelan K, Mroczek-Musulman E, and Beierle EA (2018). Targeting PIM kinase as a therapeutic strategy in human hepatoblastoma. *Oncotarget* **9**, 22665–22679.

[23] Gillory LA, Stewart JE, Megison ML, Nabers HC, Mroczek-Musulman E, and Beierle EA (2013). FAK inhibition decreases hepatoblastoma survival both in vitro and in vivo. *Transl Oncol* **6**(2), 206–215.

[24] Gillory LA, Stewart JE, Megison ML, Waters AM, and Beierle EA (2015). Focal adhesion kinase and p53 synergistically decrease neuroblastoma cell survival. *J Surg Res* **196**(2), 339–349.

[25] Faustino-Rocha A, Oliveira PA, Pinho-Oliveira J, Teixeira-Guedes C, Soares-Maia R, da Costa RG, Colaço B, Pires MJ, Colaço J, and Ferreira R, et al (2013). Estimation of rat mammary tumor volume using caliper and ultrasonography measurements. *Lab Anim (NY)* **42**(6), 217–224.

[26] Keeton EK, McEachern K, Dillman KS, Palakurthi S, Cao Y, Grondine MR, Kaur S, Wang S, Chen Y, and Wu A, et al (2014). AZD1208, a potent and selective pan-Pim kinase inhibitor, demonstrates efficacy in preclinical models of acute myeloid leukemia. *Blood* **123**(6), 905–913.

[27] Koo BS, Lee SH, Kim JM, Huang S, Kim SH, Rho YS, Bae WJ, Kang HJ, Kim YS, and Moon JH, et al (2015). Oct4 is a critical regulator of stemness in head and neck squamous carcinoma cells. *Oncogene* **34**(18), 2317–2324.

[28] Lu Y, Zhu H, Shan H, Lu J, Chang X, Li X, Lu J, Fan X, Zhu S, and Wang Y, et al (2013). Knockdown of Oct4 and Nanog expression inhibits the stemness of pancreatic cancer cells. *Cancer Lett* **340**(1), 113–123.

[29] Narita K, Matsuda Y, Seike M, Naito Z, Gemma A, and Ishiwata T (2014). Nestin regulates proliferation, migration, invasion and stemness of lung adenocarcinoma. *Int J Oncol* **44**(4), 1118–1130.

[30] Neradil J and Veselska R (2015). Nestin as a marker of cancer stem cells. *Cancer Sci* **106**(7), 803–811.

[31] Murakami S, Ninomiya W, Sakamoto E, Shibata T, Akiyama H, and Tashiro F (2015). SRY and OCT4 are required for the acquisition of cancer stem cell-like properties and are potential differentiation therapy targets. *Stem Cells* **33**(9), 2652–2663.

[32] Kuo KK, Lee KT, Chen KK, Yang YH, Lin YC, Tsai MH, Wuputra K, Lee YL, Ku CC, and Miyoshi H, et al (2016). Positive feedback loop of OCT4 and c-JUN expedites cancer stemness in liver cancer. *Stem Cells* **34**(11), 2613–2624.

[33] Jensen JB and Parmar M (2006). Strengths and limitations of the neurosphere culture system. *Mol Neurobiol* **34**(3), 153–161.

[34] Wang T, Shigdar S, Gantier MP, Hou Y, Wang L, Li Y, Shamaileh HA, Yin W, Zhou SF, and Zhao X, et al (2015). Cancer stem cell targeted therapy: progress amid controversies. *Oncotarget* **6**(42), 44191–44206.

[35] Yin S, Li J, Hu C, Chen X, Yao M, Yan M, Jiang G, Ge C, Xie H, and Wan D, et al (2007). CD133 positive hepatocellular carcinoma cells possess high capacity for tumorigenicity. *Int J Cancer* **120**(7), 1444–1450.

[36] Costantini S, Di Bernardo G, Cammarota M, Castello G, and Colonna G (2013). Gene expression signature of human HepG2 cell line. *Gene* **518**(2), 335–345.

[37] Bahnassy AA, Fawzy M, El-Wakil M, Zekri AR, Abdel-Sayed A, and Sheta M (2015). Aberrant expression of cancer stem cell markers (CD44, CD90, and CD133) contributes to disease progression and reduced survival in hepatoblastoma patients: 4-year survival data. *Transl Res* **165**(3), 396–406.

[38] Schmohl JU and Vallera DA (2016). CD133, selectively targeting the root of cancer. *Toxins (Basel)* **8**(6).

[39] Ning ST, Lee SY, Wei MF, Peng CL, Lin SY, Tsai MH, Lee PC, Shih YH, Lin CY, and Luo TY, et al (2016). Targeting colorectal cancer stem-like cells with anti-CD133 antibody-conjugated SN-38 nanoparticles. *ACS Appl Mater Interfaces* **8**(28), 17793–17804.

[40] Rabinovich GA, Gabrilovich D, and Sotomayor EM (2007). Immunosuppressive strategies that are mediated by tumor cells. *Annu Rev Immunol* **25**, 267–296.

[41] Wang Y, Chen M, Wu Z, Tong C, Dai H, Guo Y, Liu Y, Huang J, Lv H, and Luo C, et al (2018). CD133-directed CAR T cells for advanced metastasis malignancies: A phase I trial. *Oncoimmunology* **7**(7)e1440169.

[42] Zhao J (2016). Cancer stem cells and chemoresistance: The smartest survives the raid. *Pharmacol Ther* **160**, 145–158.

[43] Abdullah LN and Chow EK (2013). Mechanisms of chemoresistance in cancer stem cells. *Clin Transl Med* **2**(1), 3.

[44] Lau EY, Ho NP, and Lee TK (2017). Cancer stem cells and their microenvironment: biology and therapeutic implications. *Stem Cells Int* **2017**, 3714190.

[45] Decker S, Finter J, Forde AJ, Kissel S, Schwaller J, Mack TS, Kuhn A, Gray N, Follo M, and Jumaa H, et al (2014). PIM kinases are essential for chronic lymphocytic leukemia cell survival (PIM2/3) and CXCR4-mediated microenvironmental interactions (PIM1). *Mol Cancer Ther* **13**(5), 1231–1245.

[46] Ahirwar DK, Nasser MW, Ouseph MM, Elbaz M, Cuitiño MC, Kladney RD, Varikuti S, Kaul K, Satoskar AR, and Ramaswamy B, et al (2018). Fibroblast-derived CXCL12 promotes breast cancer metastasis by facilitating tumor cell intravasation. *Oncogene* **37**(32), 4428–4442.

[47] Larzabal L, El-Nikhely N, Redrado M, Seeger W, Savai R, and Calvo A (2013). Differential effects of drugs targeting cancer stem cell (CSC) and non-CSC populations on lung primary tumors and metastasis. *PLoS One* **8**(11)e79798.

[48] Walenkamp AME, Lapa C, Herrmann K, and Wester HJ (2017). CXCR4 Ligands: The Next Big Hit? *J Nucl Med* **58**(Suppl. 2), 77S–82S.

[49] Zhang H, Chang WJ, Li XY, Zhang N, Kong JJ, and Wang YF (2014). Liver cancer stem cells are selectively enriched by low-dose cisplatin. *Braz J Med Biol Res* **47**(6), 478–482.